

# MATHEMATICAL MORPHOLOGY IN COLOR SPACES APPLIED TO THE ANALYSIS OF CARTOGRAPHIC IMAGES

Jesús ANGULO, Jean SERRA  
Centre de Morphologie Mathématique - Ecole des Mines de Paris  
35, rue Saint-Honoré, 77305 Fontainebleau, FRANCE  
[angulo@cmm.ensmp.fr](mailto:angulo@cmm.ensmp.fr), [serra@cmm.ensmp.fr](mailto:serra@cmm.ensmp.fr)

## ABSTRACT

Automatic analysis of cartographic images is an important task for the development of intelligent geographical information systems. Both geometrical features and color are powerful cues to extract spatial semantic objects. This contribution deals with the use of the various color pieces of information for partitioning color images and for extracting geometrical-color features with mathematical morphology operators.

## KEY WORDS

Cartographic images, color image processing, mathematical morphology, connections, watershed segmentation, color top-hat, color gradient

## 1 INTRODUCTION

Automatic analysis of cartographic images is an important task for the development of intelligent geographical Information Systems [11].

From an image processing viewpoint, the contents of a cartographic color map is typically composed of color regions (each color is associated to a semantic label) and of small structures, such as text, symbols, lines, etc. Therefore, both geometrical features and color are powerful cues to extract spatial semantic objects.

The extraction of these semantic elements from an image can be made manually or supported by a computer system. Many efforts are currently carried out in order to propose satisfactory solutions for the automated interpretation of cartographic images [10, 12].

We identify two main steps: on the one hand, the segmentation of the image in order to define the color regions and in order to extract the text/graphic details, and on the other hand, the character recognition with OCR, symbol identification, color indexation, etc. [21]. In this contribution, we present a method for a full image analysis of cartographic maps based on mathematical morphology operators. The approach deals with the use of the various color pieces of information for hierarchical partitioning the image into homogeneous color regions

and for extracting a binary layer of the geometrical-color details. This powerful information can be the input to the subsequent pattern recognition algorithms which are not considered in this study.

The algorithms are illustrated by means of some examples of color cartographic images, Figure 1.



Figure 1. The color cartographic images  $f$  used in the examples.

The rest of the paper is structured as follows. First, the choice of a suitable color space for morphological image processing is discussed in Section 2. In Section 3 a reminder of the problem arising from the application of mathematical morphology to color images is included. We continue in Section 4 with a new extension of two morphological operators to color images. Then, in Section 5 are given the algorithms of our approach for the analysis of cartographic images. Finally, conclusions are included in Section 6.

## 2 COLOR SPACES FOR IMAGE PROCESSING

The choice of a suitable color space representation is still a challenging task in the processing and analysis of color images. The RGB color representation has some drawbacks: components are strongly correlated, lack of human interpretation, non uniformity, etc. A recent study [9] has shown that many color spaces (HLS, HSV,...) having been developed for computer graphic applications, are unsuited to image processing. A convenient representation must yield distances, or norms, and provide independence between chromatic and achromatic components [19]. In our works, we adopt an improved family of HLS systems that satisfy these prerequisites. This family of spaces is named: *Improved HLS* (IHLS).

There are three versions of IHLS: using the norm  $L_1$ , the norm  $L_2$  or the norm  $\max \rightarrow \min$ . The equations of transformation between RGB and the new HLS systems are given in [9] [19] and summarized in [2].

For the sake of simplicity, all the examples of the paper were obtained according to the equations:  $L = 0.212R + 0.715G + 0.072B$ ,  $S = \max(R, G, B) - \min(R, G, B)$ ,

$$H' = \arccos \left[ \frac{R - 1/2G - 1/2B}{(R^2 + G^2 + B^2 - RG - RB - GB)^{1/2}} \right], \Rightarrow H = 360^\circ - H'$$

if  $B > G$ ,  $H = H'$  otherwise.

We would like also to compare it with the  $L^*a^*b^*$  color space. The principal advantage of the  $L^*a^*b^*$  space is its perceptual uniformity. However, the transformation from the RGB to  $L^*a^*b^*$  space is done by first transforming to the XYZ space, and then to the  $L^*a^*b^*$  space [23]. The XYZ coordinates are depending on the device-specific RGB primaries and on the white point of illuminant. In most of situations, the illumination conditions are unknown and therefore a hypothesis must be made. We propose to choose the most common option: the CIE  $D_{65}$  daylight illuminant.

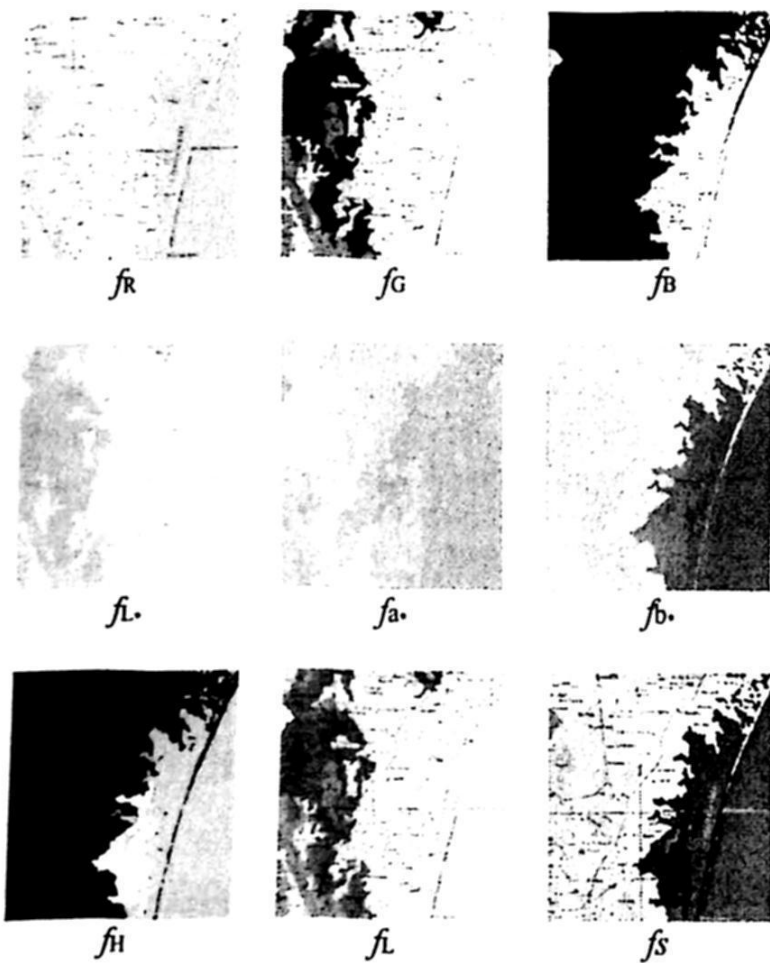


Figure 2. Color components of an image example (Figure 1(b)) in the RGB, the  $L^*a^*b^*$  and the Improved HLS color spaces.

Let  $f = (f_R, f_G, f_B)$  be a color image, its grey-level components in the improved HLS color space are  $(f_H, f_L, f_S)$  and in the  $L^*a^*b^*$  color space are  $(f_L, f_a, f_b)$ . In Figure 2 are given the different color components of an image example.

### 3 MATHEMATICAL MORPHOLOGY AND COLOR IMAGES

Mathematical morphology is the application of lattice theory to spatial structures [16]. First introduced as a shape-based tool for binary images, mathematical morphology has become a very powerful non-linear image analysis technique with operators for the segmenting, filtering and feature extraction in grey-scale images. Formally, the definition of morphological operators needs a totally ordered complete lattice structure: there are no pair of points for which the order is uncertain. Therefore, the application of mathematical morphology to color images is difficult due to the vectorial nature of the color data.

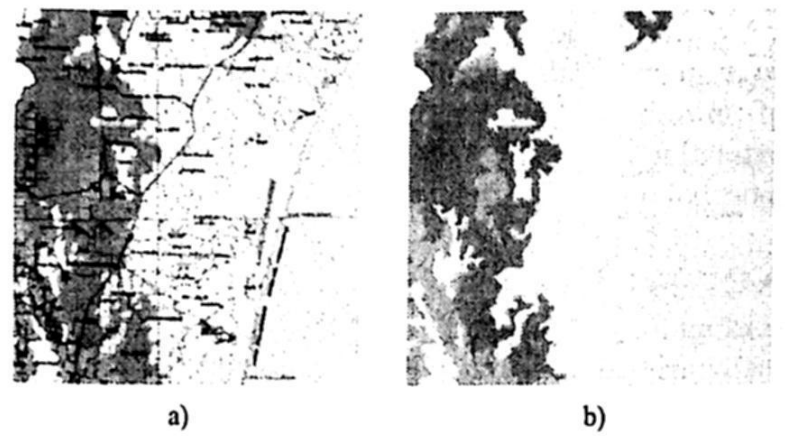


Figure 3. Example of morphological color filtering by vectorial connected operators ( $f$  is the image on Figure 1(b)): (a) Opening by reconstruction,  $\varphi_{\Omega}^{rec}(f)$ , and (b) closing by reconstruction  $\varphi_{\Omega}^{rec}(f)$ . The structuring element is a square of size  $\_$  and the lexicographical order is  $\Omega \equiv (L|_{\alpha=10} \rightarrow S \rightarrow H_{h_0} = o^a$ .

We have proposed a flexible method for the implementation of morphological vector operators in complete totally ordered lattices by using lexicographical orders which are defined on the RGB color space and on the improved HLS system [3]. In Figure 3 are shown a color opening and a color closing of a cartographic image using one of the lexicographic orders presented in [3].

The inconvenient of the vector approach is the computational complexity of the algorithms which leads to slow implementations. Moreover, different choices must be made in the lexicographical orders: priority of components, degree of influence of the components, etc.

A second drawback, more specific, deals with the processing of the hue component, i.e. with data that are defined on the unit circle [7].

However, in practice, for many applications (e.g. segmentation and feature extraction) the total orders are not required as well as increment based operators (e.g. gradients and top-hats) may be used for the hue component. Hanbury and Serra [7] have developed the application of morphological operators on the unit circle and more precisely, they have defined the circular centered gradient and the circular centered top-hat.

Another recent study [18] proposes a theory where the segmentation of an image is defined as the maximal partition of its space of definition, according to a given criterion. See also [20]. The criterion cannot be arbitrary and permits to maximize the partition if and only if the obtained classes are connected components of some connection (*connective criterion*). Therefore, the choice of a connection induces specific segmentation. In this paper, we adopt this framework and we investigate different connections for segmenting the cartographic color images.

## 4 COLOR GRADIENTS AND COLOR TOPHATS

We introduce in this section the extension of the gradient and the top-hat notions to color images.

### 4.1 GRADIENT

The color gradient function of a color image  $f$  at the point  $x$ , denoted  $\nabla f(x)$ , is associated to a measure of color dissimilarity or distance between the point and the set of neighbors at distance one from  $x$ ,  $K(x)$ . For our purposes, three definitions of gradient have been used,

- **Morphological gradient,  $\nabla f(x)$** : This is the standard morphological (Beucher algorithm [15]) gradient for grey level images ( $f: E \rightarrow T$ , where  $E$  is an Euclidean or digital space and  $T$  is an ordered set of grey-levels),  $\nabla f(x) = \delta_k(f) - \varepsilon_k(f)$ .
- **Circular centered gradient,  $\nabla_c a(x)$** : If  $a(x)$  is a function containing angular values ( $a: E \rightarrow C$ , where  $C$  is the unit circle), the circular gradient is calculated by the expression [7],  $\nabla_c a(x) = \vee[a(x) \div a(y), y \in K(x)] - \wedge[a(x) \div a(y), y \in K(x)]$  where  $a \div a' = |a - a'|$  iff  $|a - a'| \leq 90^\circ$  and  $a \div a' = 180^\circ - |a - a'|$  iff  $|a - a'| > 90^\circ$ .
- **Euclidean gradient,  $\nabla_E f(x)$** : Very interesting for vectorial functions ( $f(x) = (f_1(x) \dots f_n(x))$ ), it is based on computing the Euclidean distance  $d_E$ ,  $\nabla_E f(x) = \vee[d_E(x, y), y \in K(x)] - \wedge[d_E(x, y), y \in K(x)]$

We define a series of gradients for a color image:

1. **Luminance gradient**:  $\nabla^L f(x) = \nabla f_L(x)$
2. **Hue circular gradient**:  $\nabla^H f(x) = \nabla_c f_H(x)$
3. **Saturation weighing-based color gradient**:  
 $\nabla^S f(x) = f_S(x) \times \nabla_c f_H(x) + f_S^c(x) \times \nabla f_L(x)$  (where  $f_S^c$  is the negative of the saturation component);

### 4. Supremum-based color gradient ;

$$\nabla^{\text{sup}} f(x) = \vee[\nabla_c f_S(x), \nabla_c f_L(x), \nabla f_H(x)]$$

### 5. Chromatic gradient: $\nabla^c f(x) = \nabla_E(f_a + f_b)(x)$

### 6. Perceptual gradient: $\nabla^P f(x) = \nabla_E(f_L f_a + f_b)(x)$ .

In Figure 4 is depicted a comparative of the gradients of a color image. As we can see, the quality of the gradients is different. We show in Section 5 that the color gradient is a scalar function which can be used with the watershed transformation for segmenting the color images and we discuss how the different gradients perform on the segmentation results.

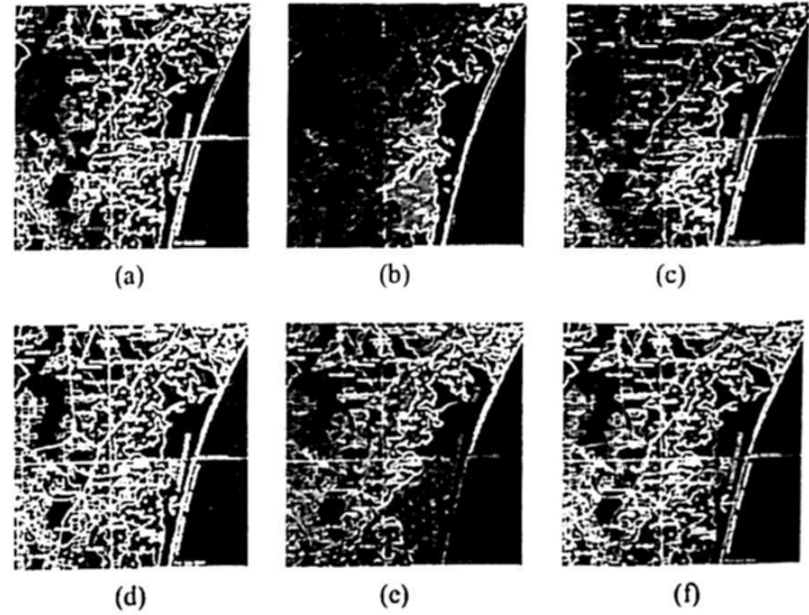


Figure 4. Examples of color gradients ( $f$  is the image on Figure 1(b)):

(a)  $\nabla^L f$ , (b)  $\nabla^H f$ , (c)  $\nabla^S f$ , (d)  $\nabla^{\text{sup}} f$ , (e)  $\nabla^c f$  and (f)  $\nabla^P f$ .

### 4.2 Top-hat

The top-hat transformation is a powerful operator which permits the detection of contrasted objects on non-uniform backgrounds. In the sense of Meyer [13], there are two versions of the top-hat (the residue between a numerical function and an opening or a closing). It involves increments and hence can be defined to circular functions like the hue component. The three definitions of top-hat used in this work are:

- **White top-hat,  $\rho_B^+(f)$** : The residue of the initial image  $f$  and an opening  $\gamma_B(f)$ , i.e.  $\rho_B^+(f) = f - \gamma_B(f)$  extracts bright structures.
- **Black top-hat,  $\rho_B^-(f)$** : The residue of a closing  $\gamma_B(f)$  and the initial image  $f$ , i.e.  $\rho_B^-(f) = \gamma_B(f) - f$ , extracts dark structures.
- **Circular centered top-hat,  $\rho_B^a(a)$** : Fast variations of an angular function (defined in the unit circle) [7], i.e.  $\rho_B^a(a) = -\sup \{ \inf [a(y) - a(x), y \in B] \}$



It is possible to define a vectorial top-hat  $\rho_B^v(f)$  (white and black) using the Euclidean distance, but this case is not considered in this paper, because we just deal with the separable top-hats in the HLS color representation.

In a similar way than the gradients, and starting from these scalar transformations, we propose three definitions for the top-hat of a color image  $f$ :

1. *White-achromatic top-hat*:  $\rho_B^{A+}(f) = \rho_B^+(f_L) \vee \rho_B^-(f_S)$

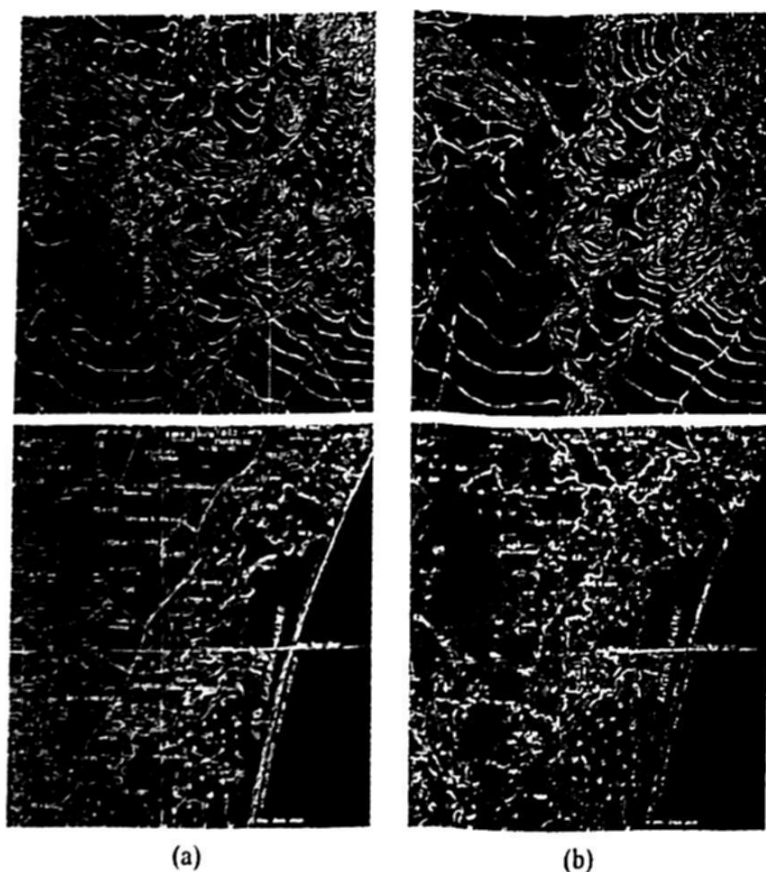
It characterizes the fast variations of bright regions (i.e. positive peaks of luminance) and the fast variations of achromatic regions on saturated background (i.e. unsaturated peaks: black, white and grey on color regions).

2. *Black-achromatic top-hat*:  $\rho_B^{A-}(f) = \rho_B^-(f_L) \vee \rho_B^+(f_S)$ .

Dually, it catches the fast variations of dark regions (i.e. negative peaks of luminance) and the fast variations of achromatic regions on saturated background (i.e. unsaturated peaks: black, white and grey on color regions).

3. *Chromatic top-hat*:  $P_B^C(f) = [f_S \times \rho_B^0(f_H)] \vee \rho_B^+(f_S)$ .

This operator extracts the fast variations of color regions on saturated color background (i.e. saturated color peaks on uniform color regions) and the fast variations of saturated color regions on achromatic (unsaturated) background (i.e. saturated color peaks on achromatic regions).



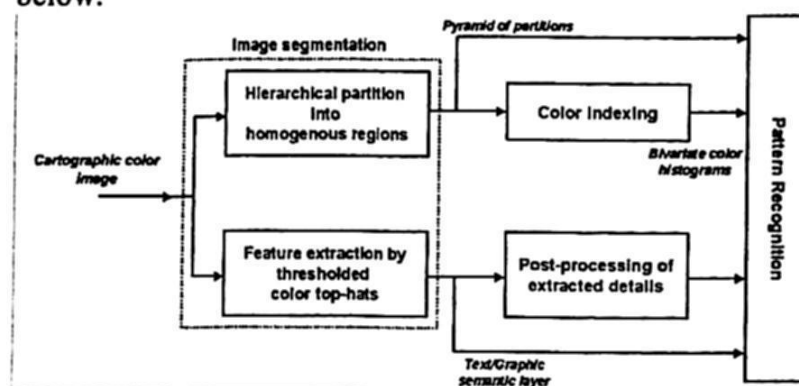
**Figure 5.** Examples of color top-hats ( $f$  are the images on Figure 1(a)-(b)): (a) Black-achromatic top-hat,  $\rho_B^{A-}(f)$  and (b) chromatic top-hat,  $\rho_B^C(f)$ . The structuring element  $B$  is a square of size 3.

Figure 5 shows the top-hat of two color images (the white-achromatic top-hat is not meaningful for these examples). We observe that the extracted objects can be different and on the other hand, a certain kind of structures are better defined on one top-hat than on the other. Their contributions are consequently complementary.

Usually, the top-hat is accompanied by a thresholding operation, in order to binarise the extracted structures. We present in Section 5 an interesting method for making the thresholding operation easier.

## 5 MORPHOLOGICAL ANALYSIS OF COLOR CARTOGRAPHIC IMAGES

The morphological approach for analyzing the color cartographic images is summarized in the overview of Figure 6. The further details of these steps are discussed below.



**Figure 6.** Overview to the proposed approach.

### 5.1 HIERARCHICAL PARTITION INTO HOMOGENEOUS REGIONS

The aim of the first step is the partitioning of the image into disjoint regions whose contents are homogeneous in color, texture, etc. In order to have a more flexible and rich approach, we propose to use a multiscale segmentation, that is, the partitioning is composed of a hierarchical pyramid with successive levels more and more simplified. In [4] we have introduced two algorithms for hierarchical color image segmentation. The first one is based on a non-parametric pyramid of watersheds, comparing different color gradients. The second segmentation algorithm relies on the merging of chromatic-achromatic partitions ordered by the saturation component. Several connections (jump connection, flat zones and quasi-flat zones) are used as connective criteria for the partitions. Both approaches involve a color space representation of type HLS, where the saturation component plays an important role in order to merge the chromatic and the achromatic information during the segmentation procedure. The presented methods are both good and fast. We would like now to evaluate the application of these algorithms to the cartographic images. We describe here the fundamentals of the algorithms and we comment on the preliminary results.

### 5.1.1 Waterfall algorithm for color images

The *watershed transformation*, a pathwise connection, is one of the most powerful tools for segmenting images. The watershed lines associate a catchment basin to each minimum of the function [5]. Typically, the function to flood is a gradient function which catches the transitions between the regions. The watershed method is meaningful only for grey tone images (is based on the existence of a total ordering relation in a complete lattice). However, it can be easily used for segmenting color images by defining a scalar gradient function corresponding to the color image. Using the watershed on a grey tone image without any preparation leads to a strong over-segmentation (large number of minima). A well-known method for avoid the over segmentation involves a non-parametric approach which is based on merging the catchment basins of the watershed image belonging to almost homogenous regions; this technique is known as *waterfall algorithm* [6].

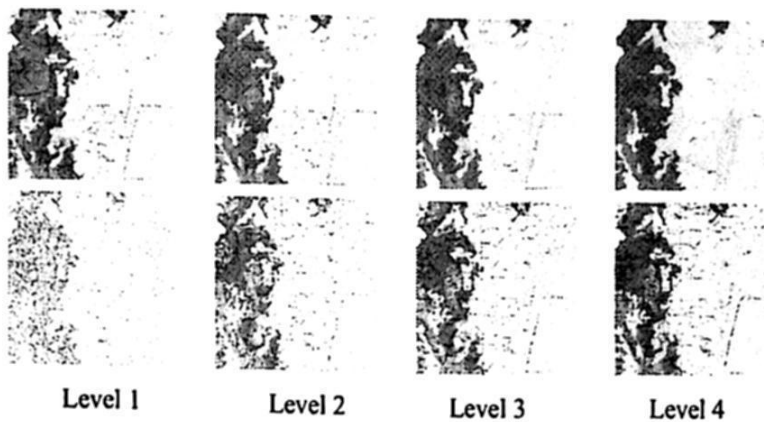


Figure 7. Pyramid of segmentation by waterfall algorithm ( $f$  is the image on Figure 1(b)). First row, mosaic images and second row, watershed lines.

Let  $g$  be a positive and bounded function ( $0 \leq g(x) \leq M$ ) and let  $W(g)$  be its watershed. An efficient algorithm for implementing the waterfalls is based on building a new function  $h$ :  $h(x) = g(x)$  iff  $x \in W(g)$  and  $h(x) = M$  ( $h$  is obviously greater than  $g$ ) and then,  $g$  is reconstructed by geodesic erosions from  $h$  [5], i.e.  $\hat{g} = R^*(g, h)$ . The minima of the resulting function  $\hat{g}$  correspond to the significant markers of the original  $g$ , moreover, the watershed transform of  $\hat{g}$  produces the catchment basins associated with these significant markers. In practice, the initial image  $g$  is the gradient of the mosaic image  $m$  (after a watershed transformation,  $m$  is obtained by calculating the average value of the function in each catchment basin). By iterating the procedure described above, a hierarchy of segmentations is obtained. Dealing with color images has the drawback of the method for obtaining the mosaic color image  $m_i$  of the level  $i$ . We propose to calculate the average values (associated to the catchment basins) in the RGB components, i.e.  $m = (m_R, m_G, m_B)$ . The gradient of level  $i+1$  is obtained from  $m_i$ , i.e.  $g_{i+1} = \nabla m_i$ . In practice, all the presented gradient functions can be applied on  $m$ . It is possible to consider a contradiction the fact that, for the mosaic image, the values are averaged in the RGB

color components and then, the gradients (and consequently the watersheds) are computed using other color components. However, this procedure of data merging allows to obtain good results and on the other hand, the calculation of the mean of angular values ( $H$ ,  $a^*$ ,  $b^*$  components) is not trivial.

The example of Figure 7 illustrates the color waterfall technique (using  $\nabla^S f$ ), with the different levels of the pyramid. The segmentation results corresponding to the different gradients are given in Figure 8. Other tests have been performed on a representative selection of color images and the results have been similar [4]. The use of only the brightness ( $\nabla^L$ ) or only the color ( $\nabla^H$  and  $\nabla^C$ ) information produces very poor results. We can observe in Figure 4 that the *supremum-based color gradient* is the most contrasted and obviously achieves to good results of segmentation. The *perceptual gradient*, which has very interesting properties for colorimetric measures in perceptually relevant units, leads to better results for the dark regions. However, the best partitions have been obtained with the proposed *saturation weighing-based color gradient*. The rationale behind this operator is the fact that the chromatic image regions correspond to high values of saturation and the achromatic regions (grey, black or white) have low values in  $f_S$  (or high values in  $f_S^C$ ). According to the expression of  $\nabla^S$ , for the chromatic regions the priority is given to the transitions of  $\nabla^H$  and for the achromatic regions the contours of  $\nabla^L$  are taken.

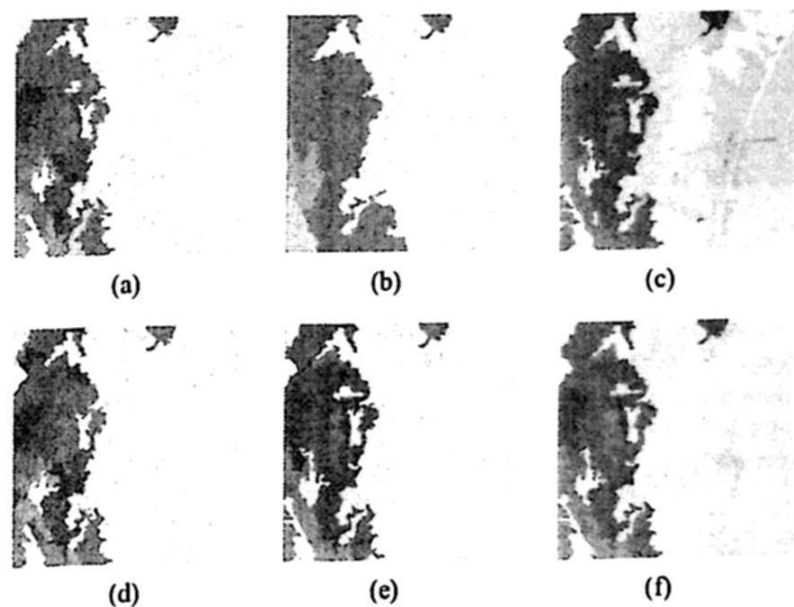


Figure 8. Examples of level 4 of waterfall pyramid using different color gradients ( $f$  is the image on Figure 1(b)): (a)  $\nabla^L f$ , (b)  $\nabla^H f$ , (c)  $\nabla^S f$ , (d)  $\nabla^{sup} f$ , (e)  $\nabla^C f$  and (f)  $\nabla^P f$ .

### 5.1.2 Ordered partition merging for color images

This segmentation approach is based on the application of other morphological connections to color images. For the sake of simplicity, we just use here the *jump connection* [17].



Let  $\sigma_k^J$  be the jump connection of module  $k$  which segments the function obtaining a partition  $P$ , i.e.  $P_{\sigma_k^J}(f)$ . The jump connection is defined for functions  $f: E \rightarrow T$  where  $T$  is a totally ordered lattice. As for the watershed, the application to color images involves special considerations. In the HLS color systems, the  $\sigma_k^J$  could be applied to each grey level component, obtaining a partition for each component, i.e.  $P_{\sigma_k^J}(f_L)$ ,  $P_{\sigma_k^J}(f_S)$ ,  $P_{\sigma_k^J}(f_H)$ . Remark that we must fix a color origin for the hue component in order to have a totally ordered set which involves some disadvantages [7]. Typically, non-significant small regions appear in the partitions (over-segmentation). The segmentation may be refined by the classical *region growing algorithm*, based on merging initial regions according to a similarity measure between them. For the region merging process, each region is defined by the mean of grey levels and the merging criterion is the *area  $a$*  of the region (regions with area smaller than  $a$  are merged to the most similar adjacent regions).

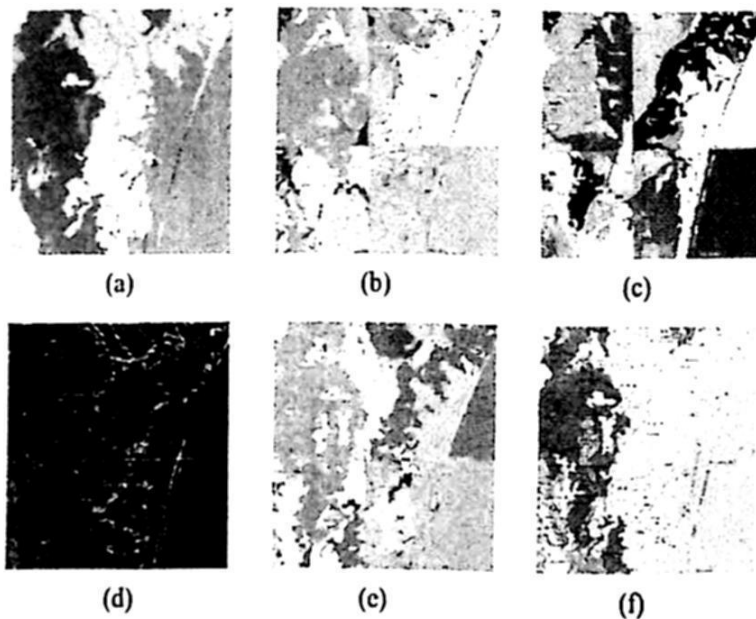


**Figure 9.** Examples of segmentation by jump connection  $k = 20 +$  region merging  $a < 50$ ,  $\sigma$ , ( $f$  is the image on Figure 1(b)): (a) Chromatic partition,  $P_{\sigma}(f_H)$ , (b) achromatic partition,  $P_{\sigma}(f_L)$ , (c) saturation partition,  $P_{\sigma}(f_S)$ , (d) saturation-based weighted contours of chromatic and achromatic partitions,  $g_s$ , (e) segmentation of weighted partition by watershed transformation,  $P_{\sigma}(f)$ , (f) contours of watershed lines on initial color image.

In Figure 9(a)-(c) are shown the partitions by jump connection improved by region merging. Now, the question is how the obtained partitions can be combined. As we can see in the example, the partition  $P_{\sigma}(f_H)$  represents well the chromatic regions (very interesting for the cartographic images), as well as  $P_{\sigma}(f_S)$  the achromatic ones. We propose the following strategy. Starting from the mosaic image associated to  $P_{\sigma}(f_S)$ , denoted  $m_S$  can use this function in order to weight the contours of the chromatic and achromatic partitions, in a similar way than for the saturation weighing-based color gradient, i.e.  $g_s(f)(x) = m_S \times P_{\sigma}(f_H)(x) + m_S^c \times P_{\sigma}(f_H)(x)$ , see Figure 9(d). The segmentation of the weighted partition  $g_s$  is obtained again by using the watershed transformation,  $P_{\sigma}(f_H) = W(g_s)$ , Figure 9(e)(f).

The increasing values of parameters  $k$  and  $a$  lead to a new pyramid of segmentation. The performance of this segmentation is relatively good. The main problem is the adequate choice of values for these parameters.

Therefore, we can conclude that for the aim of partitioning the cartographic image the most indicated method is the waterfall algorithm.

## 5.2 FEATURE EXTRACTION

The feature extraction involves basically obtaining the color top-hats which extract all the text/graphic details, as we have shown in the precedent discussion, followed by a threshold.

Now, the great difficulty arises from the binarisation of the top-hats in order to generate the semantic layer of the color image.

Besides the problem for finding the optimal threshold value, if we try the thresholding transformation directly on the top-hat image, it is probably that the result will be very noisy, Figure 10(a).

We propose to use an area opening operator. The *area opening* [22],  $\gamma_{\lambda}^a$ , is a connected filter that removes bright structures whose area is less than a give threshold  $\lambda$  but preserves the contours of the remaining objects.

Taking a size of  $\lambda = 50$ , it is possible to remove many noisy details. Moreover, the residue between this filtered image and an area opening of large size ( $\gamma_{50}^a - \gamma_{large}^a$ ) allows us to remove the background contribution, making the threshold easier, see the examples of Figure 10(b) (c).

In fact, this is also a step of segmentation (the threshold method is another connective criterion [18, 20]). We consider that the segmentation of the cartographic image is composed of the partitioning using the waterfall algorithm and the text/graphics detail extraction using the thresholded top-hats.

## 5.3 COLOR INDEXING AND POST-PROCESSING

Color is an important attribute for image retrieval: color is an intuitive feature for which it is possible to use an effective and compact representation. Color information in an image can be represented by a single 3-D histogram or three separate 1-D histograms. These color representations are invariant under rotation and translation of the image. A suitable normalization also provides scale/size invariance. The histograms are feature vectors which are used as image indices. A distance measure is used in the histogram space to measure the similarity of two images [1].

In [2], we defined two bivariate histograms:  $h_{HS}^p$ : (putting together the hue component and the saturation component) and  $h_{LS}$  (luminance and saturation components) associated to the HLS color representation. We presented an algorithm for the partitioning of these histograms using morphological tools which yields another interesting method for segmentation color images. In view of the compact representation of the chromatic-chromatic image information, the bivariate histograms are also very useful for the color distribution indexing of an image.

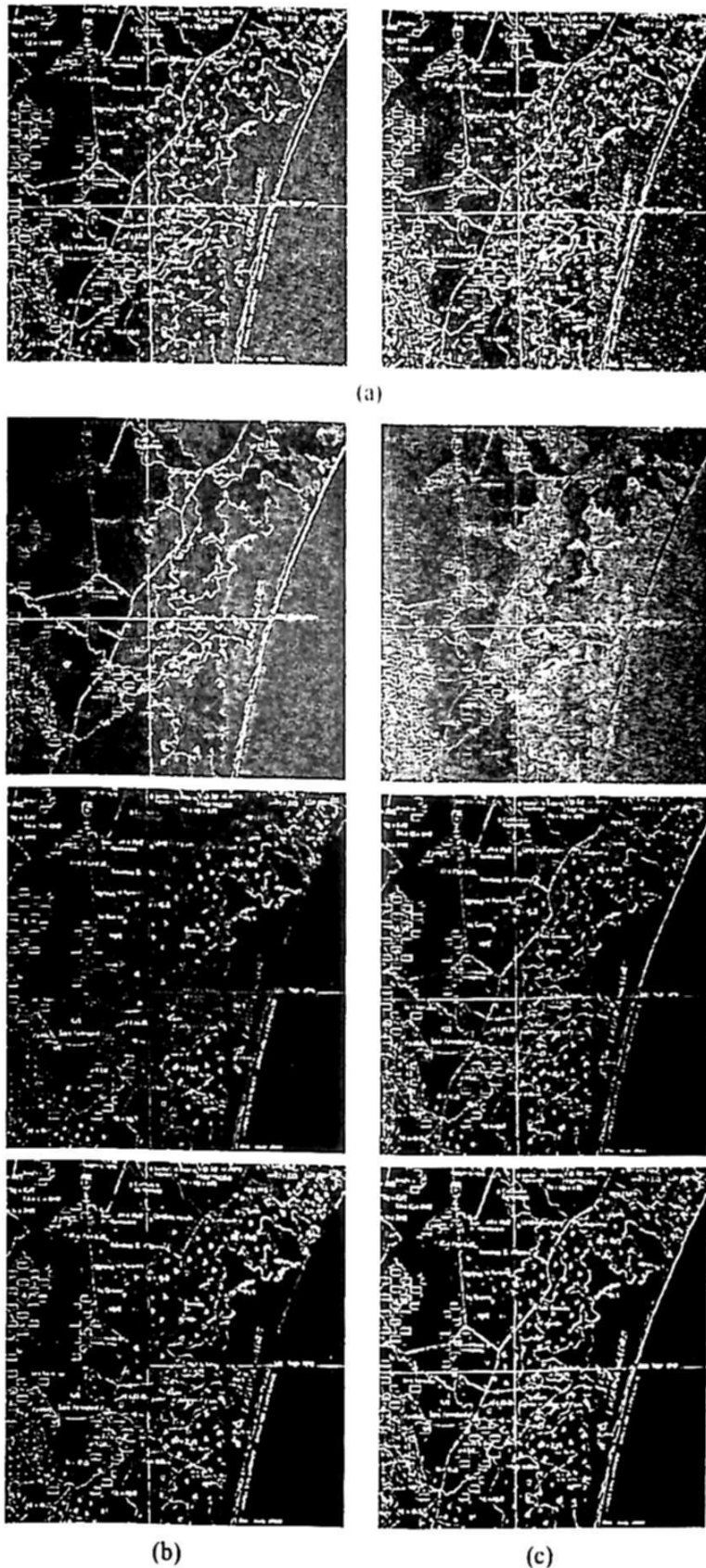


**Figure 10.** Examples of thresholding simplification by area Opening  $\gamma_{\lambda}^a$ . (a) Initial black-achromatic top-hat and binary image after thresholding at  $u = 50$ . (b) and (c) First row: area opening of size  $\lambda = 500$  and  $\lambda = 40000$ , second row: residues between the area opening of size 50 and the corresponding large area opening, third row: binary images after thresholding residues images at  $u = 50$ .

In the case of cartographic color images, one of the mosaic color images of the segmentation pyramid (where many non significant color details have been removed) can be used for computing the bivariate histograms, see Figure 11. Then, the histograms could be considered the index for a retrieval system based on the color content.



**Figure 11.** Examples of normalized bivariate color histogram images: (a) Initial image (mosaic of level 4 of the segmentation pyramid), (b) chromatic histogram  $f_{HS}$ , (c) achromatic histogram  $f_{LS}$ .

Finally, there are other morphological operators which can be applied to the binary semantic layer in order to simplify the subsequent steps of pattern recognition: for the separation between text and graphics and for the reading of the text (mainly using an OCR systems). For instance, it is possible to build the skeleton of the binary structures for better outlining the objects (characters, lines, symbols, etc). The most interesting transformation is the morphological thinning [16] which preserves the homotopy and yields robust skeletons, see examples in Figure 12.

The color of the text/graphics is also meaningful and therefore, the simple masked binary layer with the original color image constitutes an interesting information, see Figure 12.

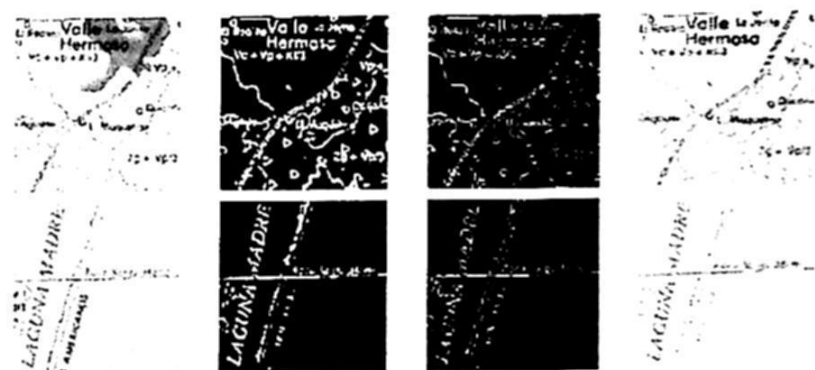


**Figure 12.** Examples of post-processing of semantic layers (first row, from the black-achromatic top-hat and second row, from the chromatic top-hat; of the image on Figure 1(b)): (a) Initial color image, (b) extracted text/graphic layer, (c) morphological thinning, (d) text/graphic layer masked with original color.

## 6 CONCLUSION

In this paper, we have proposed a new method for analysis of cartographic color images based on mathematical morphology operators. We have discussed the extension of the gradient and the top-hat notions to color images in the hue/luminance/saturation spaces. These morphological color operators can be used for hierarchical partitioning of images into homogeneous



regions and for details extraction. We also have described a technique for indexing the color distribution and for thresholding easily the extracted details.

We demonstrated on the preliminary image examples that the proposed approach is able to achieve to good segmentation results, providing robust and reproducible algorithms (very few parameters to set). We would like to evaluate deeply the performance of these techniques, comparing with other kinds of non-morphological techniques.

In summary, we believe that this approach can be used as a first step in an automated system for the management of cartographic maps in the framework of geographical information systems.

## Acknowledgements

The authors would like to thank Miguel Torres and Serguei Levachkine of the Centre for Computing Research- IPN, Mexico City, for providing the images used in this study.

## References

- [1] J. Angulo and J. Serra, Morphological color size distributions for image classification and retrieval, in *Proc. of Advanced Concepts for Intelligent Vision Systems. (ACIVS'02)*, Ghent, Belgium, September 2002.
- [2] J. Angulo and J. Serra, Segmentación de imágenes color utilizando histogramas bi-variables en espacios color en coordenadas polares," submitted to *Computación y Sistemas*, May 2003, 10 p.
- [3] J. Angulo and J. Serra, Morphological coding of color images by vector connected filters, in *Proc. 7th IEEE Int. Symp. on Signal Processing and Its Applications (ISSPA'03)*, Paris, France, July 2003.
- [4] J. Angulo and J. Serra, Color segmentation by ordered mergings, in *Proc. IEEE Conf. on Image Processing (ICIP'03)*, Barcelona, Spain, September 2003.
- [5] S. Beucher and F. Meyer, The Morphological Approach to Segmentation: The Watershed Transformation, in (E. Dougherty Ed.), *Mathematical Morphology in Image Processing*, Marcel Dekker, 433–481, 1992.
- [6] S. Beucher, Watershed, hierarchical segmentation and waterfall algorithm, in *Mathematical Morphology and Its Applications to Image Processing, Proc. ISMM'94*, pp. 69–76, Kluwer, 1994.
- [7] A. Hanbury and J. Serra, Morphological operators on the unit circle, *IEEE Transactions on Image Processing*, 10(12): 1842–1850, 2001.
- [8] A. Hanbury, Mathematical morphology in the HLS colour space, in *Proc. 12th BMVC, British Machine Vision Conference*, Manchester, pp. II-451–460, 2001.
- [9] A. Hanbury and J. Serra, A 3D-polar coordinate colour representation suitable for image analysis, submitted to *Computer Vision and Image Understanding*, November 2002, 39 p.
- [10] S. Levachkine, A. Velazquez and V. Alexandrov, Color Image Segmentation Using False Colors and Its Applications to Geo-Images Treatment: Alphanumeric Characters Recognition, in *Proc. of the IEEE International Geoscience and Remote Sensing Symposium, IGARSS'01*, Sydney, Australia, 9-13 July 2001.
- [11] S. Levachkine, A. Velazquez, V. Alexandrov and M. Kharinov, Semantic Analysis and Recognition of Raster-Scanned Color Cartographic Images, in (Blostein and Young-Bin Kwon Eds.), *Lecture Notes in Computer Science*, Vol. 2390, 178–189, Springer- Verlag, 2002.
- [12] S. Levachkine, M. Torres and M. Moreno, Intelligent Segmentation of Color Geo-Images, in *Proc. of the IEEE International Geoscience and Remote Sensing Symposium, (IGARSS'03)*, Toulouse, France, 2003.
- [13] F. Meyer, Contrast features extraction, in *Cuantitative Analysis of microstructures in Materials Science, Biology and Medicine*, Chermant, J.L. Ed., Riederer Verlag, 374–380, 1977.
- [14] F. Ortiz, F. Torres, J. Angulo and S. Puente, Comparative study of vectorial morphological operations in different color spaces, in *Proc. of Intelligent Robots and Computer Vision XX: Algorithms, Techniques, and Active Vision*, SPIE Vol. 4572, 259–268, Boston, November 2001.
- [15] J.F. Rivest, P. Soille and S. Beucher, Morphological gradients, *Journal of Electronic Imaging*, 2(4):326–336, 1993.
- [16] J. Serra, *Image Analysis and Mathematical Morphology. Vol I*, and *Image Analysis and Mathematical Morphology. Vol II: Theoretical Advances*, Academic Press, London, 1982 and 1988.
- [17] J. Serra, Connectivity for sets and functions, *Fundamenta Informaticae*, 41, 147–186, 2002.
- [18] J. Serra, Connection, Image Segmentation and Filtering, in *Proc. XI International Computing Conference (CIC'02)*, Mexico DF, November 2002.
- [19] J. Serra, Espaces couleur et traitement d'images, *CMM-Ecole des Mines de Paris*, Internal Note N-34/02/MM, October 2002, 13 p.
- [20] J. Serra, Image Segmentation, in *Proc. IEEE Conf. on Image Processing (ICIP'03)*, Barcelona, Spain, September 2003.
- [21] A. Velazquez and S. Levachkine, Text/Graphics separation and recognition in raster-scanned color cartographic maps, in *Proc. of the 5th IAPR International Workshop on Graphics Recognition, GREC'03*, 92–103, Barcelona, Spain, 2003.
- [22] L. Vincent, Grayscale area openings and closings, their efficient implementation and applications, in (Serra and Salembier Eds.), *Mathematical Morphology and its Applications to Signal Processing, Proc. ISMM'93*, UPC Publications, 22–27, 1993.
- [23] G. Wysecki and W.S. Stiles, *Color Science : Concepts and Methods, Quantitative Data and Formulae*, 2<sup>nd</sup> edition. John Wiley & Sons, New-York, 1982.